

# Modular and offsite Construction Summit

July 28-31,2025 Montreal, Canada

# Cable-Driven Parallel Robot for Module Facade Seam Sealing in Modular Construction: Static Workspace Analysis

Chen QIAN<sup>1</sup>, Xiao LI<sup>2\*</sup>, Chen SONG<sup>3</sup>, and Qianru DU<sup>4</sup>

PhD student, Department of Civil Engineering, The University of Hong Kong
 Assistant Professor, Department of Civil Engineering, The University of Hong Kong
 Research Assistant Professor, Department of Mechanical and Automation Engineering, The Chinese University of Hong Kong
 PhD student, Department of Building and Real Estate, The University of Hong Kong

Polytechnic University
\*Corresponding author's e-mail: shell.x.li@hku.hk

# **ABSTRACT**

Traditional seam sealing methods in module construction rely on workers approaching modules at height via lifting platforms or hanging baskets and using tools to seal the crevices between two modules, which are time-consuming and offer a limited workspace. This study explores the use of cable-driven parallel robots (CDPRs) to help workers achieve a wide range of seam sealing, and two cable configurations with different dimensions of CDPRs are investigated to optimize the static workspace. The results reveal that increasing the cables and the CDPRs' dimensions and controlling the platform in the center of the width side can increase their static workspace. The results suggest a potential to improve the efficiency of future seam sealing work.

# **KEYWORDS**

Module construction; Seam sealing; Cable-driven parallel robot; Static workspace

# INTRODUCTION

Modular Construction (MC), as one form of industrialized construction, has emerged as a solution to increase productivity, reduce waste, and enhance safety (Pan and Hon, 2020). Seam sealing is an important step after module assembly to help waterproof, insulate, and improve the overall stability of the modules (Orlowski et al., 2018). However, traditional seam sealing methods in MC require workers to access the modules at the height via lifting platforms or hanging baskets, which are time-consuming and offer a limited workspace (Orlowski et al., 2018). Construction robots provide an alternative to a faster, larger-scale, and safer seam-sealing process. The unpredictability of the construction site and the need to minimize disruption to the surrounding area require adaptable and compact robotic systems. The CDPRs consist of multiple flexible cables suspending the end-effector (EE) and are characterized by their compactness, large workload, and ease of reconfiguration, which promote their suitability within the constraints of a complex environment. Moreover, even if strong winds are encountered while working, the CDPR is safer because it can control the EE's pose to resist certain wind forces by controlling the cable length.

In construction, payloads can be lifted by the CDPRs, which utilize cables to control the EE pose. Calculating the CDPRs' static workspace, i.e., the EE pose that can be achieved while satisfying some specific constraints (Carricato et al., 2024), is an important step in evaluating the robot's

performance. By calculating the workspace, it can be ensured that the robot does not operate outside of safe limits, thereby reducing the risk of accidents. For effective seam sealing in a construction site, the dimensions of the CDPR frame, including its height and length, cannot surpass the dimensions of the building. The limitations imposed by the CDPRs' dimension and the restrictions on cable force culminate in a system that may make it difficult for the EE to reach the corners of the module facade. This work explores the possibility of using CDPRs to help workers achieve a wide range of seam sealing and compares the static workspace of CDPRs with different dimensions and cable configurations to maximize the workspace.

The remainder of the paper is organized as follows: A literature review of CDPRs in construction and the methods for workspace analysis are provided in the literature review section. The approaches for workspace calculations are described in the method section. The experimental evaluation is presented in the experiment section. The study's results are discussed in the discussion section. The conclusion section summarizes the conclusions of this study.

#### LITERATURE REVIEW

Existing studies have demonstrated CDPRs' potential in various construction applications, and their workspace analysis has been conducted.

# **CDPRs in Construction**

In recent years, CDPRs have been widely utilized to improve safety and efficiency in construction scenarios like transporting materials (Yang et al., 2021). Pott et al. (2010) introduced a robotic system to streamline the on-site final assembly of solar power plants. This system leverages a CDPR and offers a larger workspace. Kumar et al. (2019) examined the static workspace for a four-cable underactuated CDPR, considering the cable force and moments applied on the mobile platform. Shao et al. (2021) proposed a planar four-cable CDPR to conduct the facade cleaning of high-rise buildings. The authors analyzed the cable forces to obtain a larger workspace. Iturralde et al. (2022) utilized a CDPR to install curtain wall modules. The results show that the workspace and efficiency of the robotic curtail wall module installation surpass manual installation. To our knowledge, no prior research has explored CDPRs' application for seam sealing in MC.

# **Static Workspace Analysis**

Workspace calculation is essential to ensure the control and safety of CDPRs (Peng and Bu, 2021). Pott and Kraus (2016) designed an algorithm that can exploit different methods to speed up the wrench-closure workspace calculation of redundantly constrained CDPRs. Merlet (2016) considered workspace calculations for three cable models: straight-line cable, straight-line linear elastic cable, and sagging cable. Boumann et al. (2020) designed an approach to obtain the wrench feasible workspace for mobile CDPRs by ascertaining their available wrench set. They discovered that the mobile CDPR's wrench set depends on cable tension limits and moment equilibrium. Liu et al. (2024) explored the feasibility of CDPR for automated precast panel installation, especially in dense urban areas. Most work about workspace analysis of CDPRs has a small workspace coverage rate and requires much computation.

# Research Gap

No prior research has explored the application of CDPRs for efficient seam sealing in MC. Most existing work on the CDPR workspace did not consider the impact of different cable configurations and had a small workspace coverage rate.

# **METHOD**

This section presents the methodology for analyzing the workspace of CDPRs in seam sealing applications for modular construction.

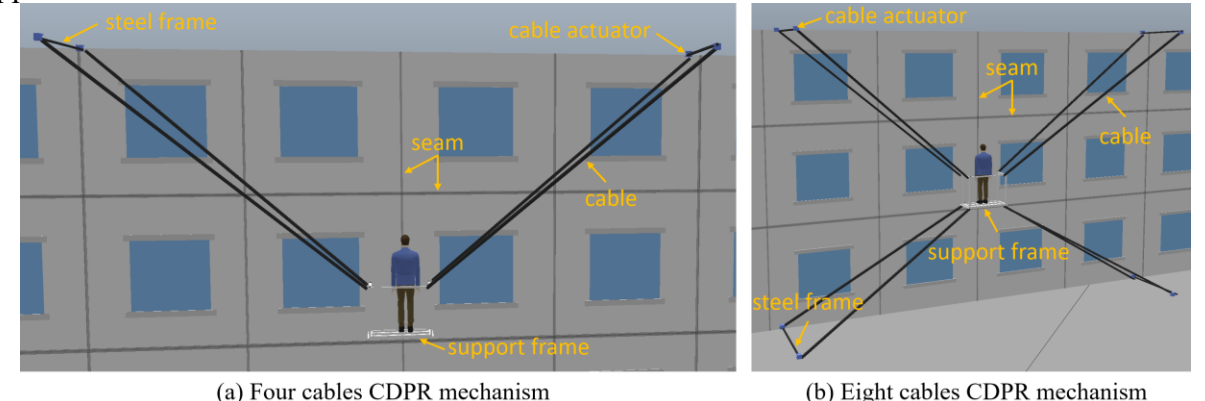
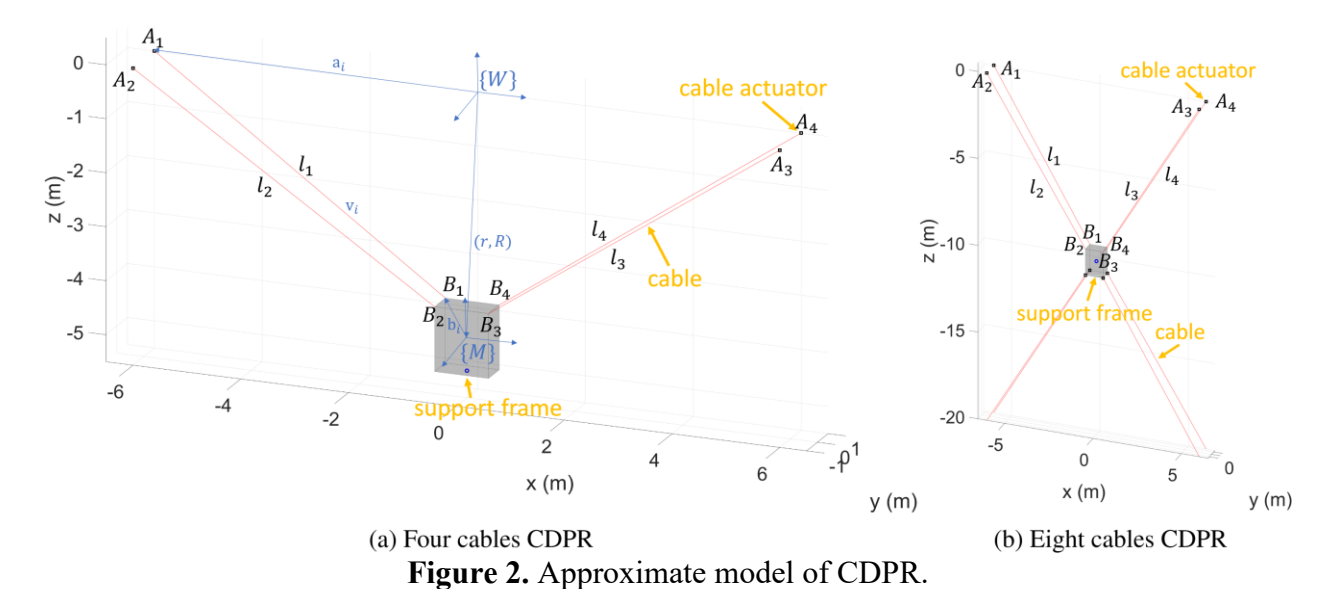


Figure 1. Seam sealing scenario in MC by using CDPR.



#### **Equivalence Model**

Figure 1(a) shows how steel frames and cable actuators are installed on the roof, and cables connect the steel frame to the support frame to ensure that the support frame is stable and stationary at the specified position. Workers stand on support frames to seal the seam between modules. As shown in Figure 2(a), an equivalence model is constructed in Matlab. The *i*th cable actuator, denoted as  $A_i$ , carries cable  $l_i$ . Similarly, Figure 1(b) shows steel frames and cable actuators are installed on the roof and ground, and an equivalent model is constructed in Matlab shown in Figure 2(b). Define  $\mathbf{v}_i$  as the unit directional vector from the attachment point  $B_i$  on the support frame to the cable exit point  $A_i$  of the actuator, and  $\mathbf{f}_i$  represents the cable tension vector set:

$$\mathbf{f}_i = f_i \mathbf{v}_i \tag{1}$$

where  $f_i$  is the cable tension of the corresponding cable  $l_i$ .

# **Kinematic Model**

The CDPR consists of three parts: the world coordinate system  $\{W\}$ , the supporting frame in the local coordinate system  $\{M\}$ , and the cable connecting the support frame to the steel frame, as shown in Figure 1(a).  $\mathbf{a}_i$  represents the vector extending from the world coordinate system's origin

to the cable actuator.  $\mathbf{b}_i$  denotes the vector connecting the local coordinate system's origin to the corner point of the support frame. The pair (r, R) indicates the relative transformation from the local coordinate system in relation to the world coordinate system:

$$l_i = \mathbf{a}_i - r - R\mathbf{b}_i \tag{2}$$

To derive the kinematic model, the force and torque equilibrium equations are solved:

$$\underbrace{\begin{bmatrix} \mathbf{v}_1 & \dots & \mathbf{v}_n \\ R\mathbf{b}_1 \times \mathbf{v}_1 & \dots & R\mathbf{b}_n \times \mathbf{v}_n \end{bmatrix}}_{\Xi^{\mathsf{T}}} \underbrace{\begin{bmatrix} f_1 \\ \vdots \\ f_n \end{bmatrix}}_{\mathbf{w}_{\mathsf{p}}} + \underbrace{\begin{bmatrix} mg \\ \tau_{\mathsf{p}} \end{bmatrix}}_{\mathbf{w}_{\mathsf{p}}} = \mathbf{0} \tag{3}$$

where m is the total mass of the support frame and the worker, g is the gravitational acceleration, and  $\tau_p$  is the torque applied to the support frame. For this particular application,  $\tau_p=0$ . Formula (3) can be transformed into a matrix-vector form as follows:

$$\Xi^T \mathbf{f} + \mathbf{w}_p = 0 \tag{4}$$

where  $\Xi^T$  is the transpose of the Jacobian matrix,  $\mathbf{f}$  is the cable force vector, and  $\mathbf{w}_p$  is the total wrench applied on the robot.

# **Static Workspace Calculation**

When the system is in static equilibrium, it must satisfy force and moment equilibrium:

$$\begin{cases} \Xi_{F}\mathbf{f} - m\mathbf{g} = \mathbf{0}_{3\times 1} \\ \Xi_{M}\mathbf{f} - \tau_{p} = \mathbf{0}_{3\times 1} \\ \mathbf{f}_{min} \leq \mathbf{f} \leq \mathbf{f}_{max} \end{cases} \tag{5}$$
 where  $\Xi_{F}$  and  $\Xi_{M}$  are the Jacobi matrices of the robot's forces and moments, respectively.  $\mathbf{f}_{min}$ 

and  $\mathbf{f}_{max}$  denote the minimum and maximum cable tensions, respectively.

The algorithm employs a position grid that covers the potential position of the support frame. Because the x- and y-direction positions of the support frame must be within the rectangular area formed by the cable actuators, the grid's x and y dimensions are the same as the rectangular area composed of cable actuators, and the z-direction dimension is the building's height. The fmincon (a function used in MATLAB to solve nonlinear optimization problems with constraints) function calculates the feasible position and checks whether the solution satisfies the forces and moments equilibrium. The steps for static workspace calculation are as follows: [1] The support frame's position limits are set by defining a bounding box with minimum and maximum coordinates:  $[x_{-}l,$  $[x_u]$ ,  $[y_l, y_u]$ , and  $[z_l, z_u]$ ; [2] The range between limits is divided by a regular grid with  $n_g$ nodes; [3] For each node within these sections, a numerical solution for the robot's static equilibrium is calculated by using the fmincon function in Matlab; [4] If a solution is obtained, the feasibility of the system is verified to ensure that the solution is viable and stable; [5] If the checks in Step 4 confirm that the solution is feasible, then the support frame's position is recorded as part of its feasible workspace.

# **EXPERIMENT**

Simulation experiments were conducted to demonstrate the algorithm's effect. In these experiments, the CDPRs in Matlab are designed in different dimensions and cable configurations to compare which type covered the most area. The experiments consist of two parts: 1) Four-cable CDPR experiments and 2) eight-cable CDPR experiments. The workspace computation algorithm was implemented in Matlab on a PC with an i9 Intel processor and 192 gigabytes of Random Access Memory (RAM).

# **Four Cables CDPR Experiments**

**Table 1.** Static workspace calculation parameters.

Parameter	Value	Unit
$A_1A_2$	2.0	m
$A_2A_3$	16.0 or 14.0 or 12.0 or 10.0 or 8.0	m
$B_1B_2$	1.0	m
$B_2B_3$	1.0	m
$x_{-}l$	-8.0 or -7.0 or -6.0 or -5.0 or -4.0	m
$x_u$	8.0 or 7.0 or 6.0 or 5.0 or 4.0	m
x_step	0.2	m
$y\_l$	-0.3	m
$y_u$	0.0	m
y_step	0.3	m
$z\_l$	-19.2	m
$z_u$	0.0	m
z_step	0.2	m
m	200.0	kg
t	15.0	٥
$f_{max}$	5,000.0	N
$f_{min}$	0.0	N

The first approximate model of CDPR is shown in Figure 2(a). According to China (1995), the maximum tilt angle safety threshold t of the support frame when carrying a person is  $15^{\circ}$ . The height and width of the supporting frame are 1.5 meters and one meter, and the distance between the platform's center and the building wall is set to be no more than one meter. This ensures that when a worker is standing at the edge of the support frame, the distance from the hand to the module is less than 0.5 meters, and its closest distance is controlled at 0.2 meters, preventing the support frame from colliding with the module façade. The average human arm length is about 0.6 meters (Chen et al., 2016), so it is a comfortable distance for human hands to complete seam sealing. The steel frame is usually installed on the top of the building during seam sealing. Due to the wear and tear on the support frame caused by the CDPR rubbing against the ground and the fact that most adults are taller than 1.6 meters (Scheffler and Hermanussen, 2022), the lowest position in the z-direction is -19.2 meters for a 20-meter-high building. The parameters of the static workspace calculation are shown in Table 1.

Changing the dimension of the CDPR can expand the static workspace. Theoretically, the dimensions can be extended in height and length, but each method has limitations. Height extensions are restricted to the height of the building and can be affected by wind loads (Liu et al., 2024). Given the constraints of densely constructed environments, length expansion offers a more favorable option due to the limitations inherent in height expansion. In this work, the length  $A_2A_3$  is changed to compare the effect of changing the length on the CDPR static workspace. The static workspace calculation results of four-cable CDPR in different lengths are shown in Figure 3, where the x-axis represents the horizontal displacement relative to the building facade, the y-axis represents the horizontal displacement relative to the steel frame, the Z-axis represents the vertical coverage range (0 to -19.2 meters for 20.0 meter-high building), and the blue aeras represent the feasible workspace positions satisfying all constraints (Eq. 5).

For ease of understanding, coverage rate w is used to denote the ratio of the static workspace area SW to the plane area P formed by the x range and the z range in the grid (e.g., when the length =

12 meters, the x range is -6 to 6, and the z range is -19.2 to 0). The polyarea function (a function used in MATLAB to calculate the area of polygons) is used to calculate the area of a polygonal static workspace. The calculation of w is shown in Table 2.

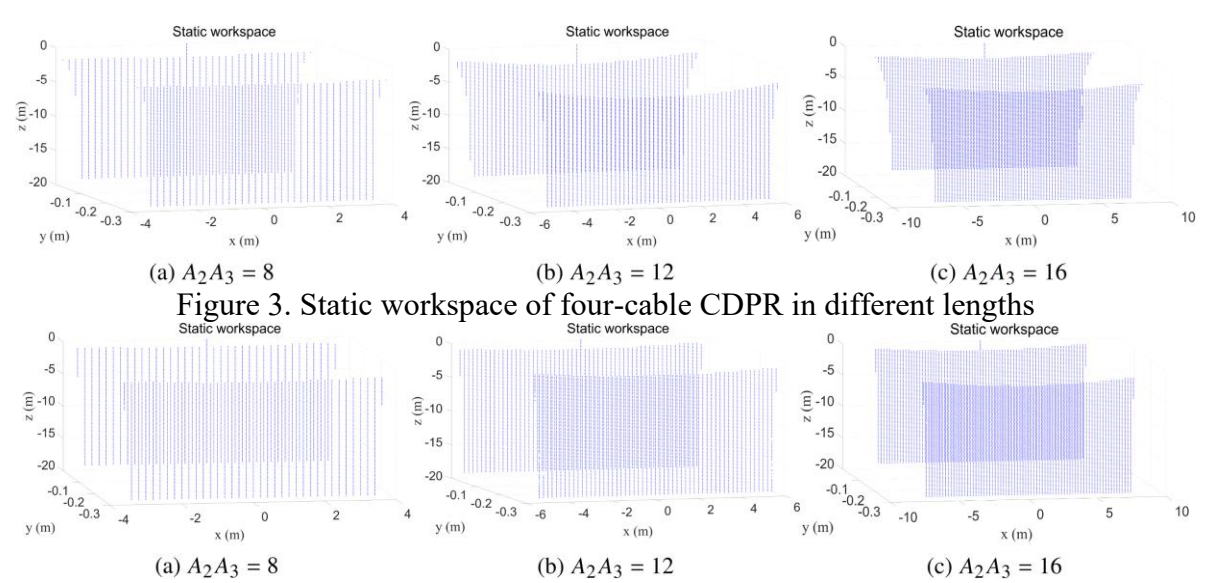


Figure 4. Static workspace of eight-cable CDPR in different lengths.

<b>Table 2.</b> Coverage rate of	CDPR fo	or different	numbers of	cables and	lengths.

Cable configuration	$A_2A_3$	у	$\overline{w}$
	16	0	0.8613
	16	-0.3	0.8383
	14	0	0.8612
Four-cable CDPR	14	-0.3	0.8286
Tour cubic CBTR	12	0	0.8497
	12	-0.3	0.8307
	10	0	0.8425
	10	-0.3	0.8156
	8	0	0.8375
	8	-0.3	0.8156
	16	0	0.9154
	16	-0.3	0.8909
	14	0	0.9071
Eight-cable CDPR	14	-0.3	0.8827
Eight their CETT	12	0	0.8960
	12	-0.3	0.8720
	10	0	0.8807
	10	-0.3	0.8570
	8	0	0.8576
	8	-0.3	0.8349

# **Eight Cables CDPR Experiments**

A more complex configuration with 8 cables and actuators is also considered in this work, seen in Figure 2(b). Different dimensions of CDPRs are also considered. The static workspace calculation results of eight-cable CDPR in different lengths are shown in Figure 4 and Table 2, respectively.

#### **DISCUSSION**

The experimental results show that the coverage rate w increases when the length of the CDPR increases. This is because the EE is easily limited by cable forces when approaching the boundary, thus reducing the workspace utilization. When the length of the CDPR increases, although this problem also occurs, the area in the center that can be fully covered increases, and the overall

coverage rate increases with a small change in the edge coverage rate. Moreover, as the distance between the cable exit points increases, the crossover and interference between the cables decrease. Under the same length condition, the coverage rate of the CDPR with eight cables is larger than that of the CDPR with four cables. In this robotic system, the EE has six degrees of freedom. If four cables connect the EE, it is an under-constrained CDPR. It is a redundantly constrained system if eight cables connect the EE. Redundantly constrained CDPRs can better distribute and optimize cable force to avoid overloading or failure of a single cable. This optimized force distribution improves system reliability and workspace utilization (Pott and Bruckmann, 2013). When the ycoordinate of the support frame is away from 0, the force and torque distribution of the cables can become uneven. This can lead to overloading some cables, while others may slacken, reducing the stability and control accuracy of the system, reducing the accessible workspace (Mattioni et al., 2022). Figures 3 and 4 show how the worker support platform can cover a range of workspaces, following a 'Z' trajectory from top to bottom of the building. This is more efficient than using lifting platforms or hanging baskets where workers can only work in a vertical direction. The algorithm's computational complexity is  $O(n^3)$  because three nested loops traverse all the position points in the grid. When using Matlab in the simulation experiments, the workspace for the CDPR is available within five minutes. the structure of the CDPRs can also be extended to other practical modular applications, including curtain wall installation, prefabricated panel spraying operations, and structural inspection tasks.

In future work, more cable configurations can be attempted to achieve a larger workspace. For example, it is possible to have the cables connect different corners of the support frame while ensuring no collision between the cables.

# **CONCLUSION**

This paper explored the use of CDPRs to facilitate more convenient seam sealing in MC, and two cable configurations of the CDPR with different dimensions are explored to maximize the static workspace. The results show that increasing the number of cables, expanding the length dimension of the CDPR, and positioning the platform at the center of the width side can increase their static workspace. The findings indicate that CDPRs can potentially improve the efficiency of future seam sealing work. More complex cable configurations will be considered to achieve a larger workspace.

# **ACKNOWLEDGMENTS**

We thank Dr. Chen SONG for providing the model in Figure 2(a).

#### **REFERENCES**

- Boumann, R., Lemmen, P., Heidel, R., & Bruckmann, T. (2020). Optimization of trajectories for cable robots on automated construction sites. *In ISARC. Proceedings of the International Symposium on Automation and Robotics in Construction*, 37, 465–472. IAARC Publications. DOI: 10.1007/978-952-94-3634-7\_41
- Carricato, M. (2024). Static workspace computation for underactuated cable-driven parallel robots. *Mechanism and Machine Theory*, 193, 105551. DOI: 10.1016/j.mechmachtheory.2023.105551
- Chen, Z., Key, T., Smith, M., Woodward, M., & Collaboration, N. R. F., et al. (2016). A century of trends in adult human height. *Elife*, 5(e13410). DOI: 10.7554/eLife.13410
- China (1995). *National Standard of the People's Republic of China*. Department of Standards and Norms, Ministry of Construction of the People's.

- Iturralde, K., Feucht, M., Illner, D., Hu, R., Pan, W., Linner, T., Bock, T., Eskudero, I., Rodriguez, M., & Gorrotxategi, J., et al. (2022). Cable-driven parallel robot for curtain wall module installation. *Automation in Construction*, 138:104235. DOI: 10.1016/j.autcon.2022.104235
- Kumar, A., Antoine, J., Zattarin, P., & Abba, G. (2019). Workspace Analysis of a 4 Cable-Driven. In ROMANSY 22–Robot Design, Dynamics and Control: Proceedings of the 22<sup>nd</sup> CISM IFTOMM Symposium, 2018, 584, p. 204. Springer. DOI: 10.1007/978-3-319-78963-7 27
- Liu, Y., Zhang, R., Hayes, N., Hun, D. E., & Maldonado Puente, B. (2024). Cable-driven parallel robot (cdpr) for panelized envelope retrofits: Feasible workspace analysis. Technical report, Oak Ridge National Laboratory (ORNL), Oak Ridge, TN (United States). DOI: 10.22260/ISARC2024/0140
- Mattioni, V., Idà, E., & Carricato, M. (2022). Force-distribution sensitivity to cable-tension errors in overconstrained cable-driven parallel robots. *Mechanism and Machine Theory*, 175:104940. DOI: 10.1016/j.mechmachtheory.2022.104940
- Merlet, J.-P. (2016). On the workspace of suspended cable-driven parallel robots. In 2016 IEEE International Conference on Robotics and Automation (ICRA), 841–846. IEEE. DOI: 10.1109/ICRA.2016.7487214
- Orlowski, K., Shanaka, K., & Mendis, P. (2018). Design and development of weatherproof seals for prefabricated construction: A methodological approach. *Buildings*, 8(9):117. DOI: 10.3390/buildings8090117
- Pan, W. & Hon, C. K. (2020). Briefing: Modular integrated construction for high-rise buildings. *Proceedings of the Institution of Civil Engineers-Municipal Engineer*, 173, 64–68. Thomas Telford Ltd. DOI: 10.1680/jmuen.18.00028
- Peng, Y. & Bu, W. (2021). Workspace analysis of planar suspended two-cable-driven parallel robots. *International Conference on Mechanical Design*, 1153–1168. Springer. DOI: 10.1007/978-981-16-7381-8 72
- Pott, A. & Bruckmann, T. (2013). Cable-driven parallel robots. Springer. DOI: <u>10.1007/978-3-319-76138-1</u>
- Pott, A. & Kraus, W. (2016). Determination of the wrench-closure translational workspace in closed-form for cable-driven parallel robots. In 2016 IEEE International Conference on Robotics and Automation (ICRA), 882–887. IEEE. DOI: 10.1109/ICRA.2016.7487218
- Pott, A., Meyer, C., & Verl, A. (2010). Large-scale assembly of solar power plants with parallel cable robots. *ISR 2010 (41<sup>st</sup> International Symposium on Robotics) and ROBOTIK 2010 (6<sup>th</sup> German Conference on Robotics)*, 1–6. VDE. DOI: 10.1109/ISR.2010.5756909
- Scheffler, C. & Hermanussen, M. (2022). Stunting is the natural condition of human height. *American Journal of Human Biology*, 34(5):e23693. DOI: 10.1002/ajhb.23693
- Shao, Z., Xie, G., Zhang, Z., & Wang, L. (2021). Design and analysis of the cable-driven parallel robot for cleaning exterior wall of buildings. *International Journal of Advanced Robotic Systems*, 18(1):1729881421990313. DOI: 10.1177/1729881421990313
- Yang, G., Wang, S., Okamura, H., Shen, B., Ueda, Y., Yasui, T., Yamada, T., Miyazawa, Y., Yoshida, S., & Inada, Y. (2021). Hallway exploration-inspired guidance: Applications in autonomous material transportation in construction sites. *Automation in Construction*, 128:103758. DOI: 10.1016/j.autcon.2021.103758